Film formation and surface growth on tin electrodes in bicarbonate solutions: An impedance spectroscopy study

Article *in* Corrosion Science · March 2005

DOI: 10.1016/j.corsci.2004.07.017

CITATIONS
5

READS
6

5 authors, including:

S. H. Bonilla
Universidade Paulista
59 PUBLICATIONS **611** CITATIONS
SEE PROFILE

Javier Ernesto Rodríguez Yáñez
Universidad Estatal a Distancia
15 PUBLICATIONS **82** CITATIONS
SEE PROFILE

Available online at www.sciencedirect.com
SCIENCE DIRECT®
Corrosion Science 47 (2005) 835–848
CORROSION SCIENCE
www.elsevier.com/locate/corsci

Film formation and surface growth on tin electrodes in bicarbonate solutions: an impedance spectroscopy study

S.H. Bonilla [a], J. Rodriguez [b], C.F. Zinola [b], C. Bello [c], B.F. Giannetti [a,*]

[a] *Laboratório de Fisicoquímica Teórica e Aplicada, LaFTA, Instituto de Ciências Exatas e Tecnologia, Universidade Paulista, Dr. Bacelar 1212, CEP 04026 002 São Paulo, SP, Brazil*
[b] *Laboratorio de Electroquímica Fundamental, Facultad de Ciencias, Universidad de la República, Iguá 4225, CP 11400 Montevideo, Uruguay*
[c] *Unidad Central de Instrumentación Científica (UCIC), Facultad de Ciencias, Universidad de la República, Iguá 4225, CP 11400 Montevideo, Uruguay*

Available online 20 August 2004

Abstract

The electrochemical behaviour of potentiodynamically formed thin anodic films of polycrystalline tin in aqueous sodium bicarbonate solutions (pH ≈ 8.3) were studied using cyclic voltammetry and electrochemical impedance spectroscopy. Different equivalent circuits corresponding to various potential regions were employed to account for the electrochemical processes taking place under each condition.

Keywords: A. Tin; B. EIS; B. Cyclic voltammetry; C. Anodic film

* Corresponding author.
E-mail address: biafgian@unip.br (B.F. Giannetti).

0010-938X/$ - see front matter © 2004 Elsevier Ltd. All rights reserved.
doi:10.1016/j.corsci.2004.07.017

1. Introduction

The aim of this work was the study of initial stages and growth of thin films on tin as well as their reductive processes in slightly alkaline solution at pH 8.3. This pH value was chosen since solubility of various tin oxides and hydroxides present a minimum (remember the amphoteric nature of the metal), leading to a more stable situation. The main emphasis of the paper is to interpret the electrochemical impedance spectroscopic results, using the electrical equivalent circuit (EC) approach. Motivation arises from two necessities. First of all, the need of completing the information related to tin electrochemical behaviour in bicarbonate medium already obtained mainly from voltammetric studies both in quiescent solution and with rotating disk electrodes [1]. Secondly, the very promissory properties of tin electrodes showed in the environmental perchlorate remediation where the metal acts as an electrocatalyst for perchlorate reduction [2]. Perchlorate concentration in drinking water have surpassed safety levels in the proximity of weapon and aerospace material industries at the USA [3]. In this way, the use of tin electrodes offers a clean technology to deal with the problem. Electrochemical results showed that the extent of the reduction process of interest is highly dependent on the surface state [2]. It was cited that previous oxidation of the electrode surface resulted in the increase of the reduction of perchlorate current [2]. Thus, the improving of our knowledge about the electrical properties of the films formed on tin during oxidation will be of great importance.

2. Experimental details

An AUTOLAB equipment, PGSTAT 20 model (with the FRA module), was used to perform the electrochemical measurements. A standard electrochemical cell with an input for N_2 bubbling was used. The experiments were performed using a tin disk of 0.25 cm (electrode A) or 0.1 cm diameter (electrode B) mounted in polyester resin. The reference electrode was Ag/AgCl placed in a Luggin–Haber capillary and the counter electrode was a cylindrical platinum grid placed around the working electrode. The auxiliary electrode was a large area one since its impedance must be neglected in comparison with the impedance of a working electrode. The electrolyte, 0.5 mole l^{-1} sodium bicarbonate solution, pH $\approx$ 8.3, was prepared from Aldrich p.a. grade reagent and Millipore-MilliQ water. Before each experiment, the tin electrode surface was wet-ground with abrasive grade 600-mesh paper, washed with Millipore-MilliQ water, immersed in the electrolyte and cathodically polarised at -1.8 V during 60 s. Potential values quoted in this text are referred to the Ag/AgCl reference electrode scale. All the experiments were carried out at 25 °C.

The films were potentiodynamically grown and the scan was performed at a scan rate of $v = 0.2\ V\,s^{-1}$ up to the selected potential value, stated in the text for each case. At this potential the impedance measurements were initiated after 30 s of equilibration time in order to attain current stabilization. Current values are also accompanied during the experiments. The acquisition of electrochemical impedance data

was carried out in the 10 kHz $\leqslant f \leqslant$ 10 mHz (sometimes the interval was extended until 1 mHz) and the amplitude of the signal was 10 mV. Impedance measurements were also performed in order to characterise the reduction processes. The procedure was as follows: (i) potentiodynamically formation of the film as a result of a positive scan at $v = 0.2\ \mathrm{V\,s^{-1}}$ until the pre-set positive limit; (ii) reversal of the sweep and voltammetric profile until the attainment of the maximum of the cathodic peak. After then, the spectrum was performed at the maximum of the cathodic peak, after 30 s of equilibration time. All the voltammetric curves were recorded at $0.2\ \mathrm{V\,s^{-1}}$. The lower ($E_{\lambda c}$) and the upper scan limits ($E_{\lambda a}$) are stated in each case. To perform impedance measurements it is necessary to be certain that the system is under steady-state conditions. The examination of chronoamperometric measurements enables us to affirm that the constraint was satisfied.

Also impedance measurements were carried out in order to characterise the interface obtained after the application of potentiostatic ageing procedures. The potentiostatic ageing methodology described by Arvia [4], consisted of the implementation of a potential scan until the attainment of an ageing potential, $E\tau$, where the scan was stopped and the potential hold during a time lapses (τ). The scan is then re-initiated and the recorded profile compared with the typical voltammogram.

The Boukamp software [5] (included in the AUTOLAB software) was used to determine the equivalent circuits. For some cases a self-made programme in MATLAB was employed to fit data. The methodology employed to select the equivalent circuit was initiated with the establishment of a simple model that represents the interface. The latter was selected based on the information about the possible physical phenomena (gained in previous studies). At a next step, and if the results were not satisfactory, additional circuit elements were added to the account for other factors. The nomenclature adopted to describe the electrical circuits was the one proposed by Boukamp.

3. Results and discussion

3.1. General considerations

The typical cyclic voltammogram of tin in bicarbonate medium (shown in Fig. 1) is similar to those found in the literature for the same condition of pH interval [6–11]. However, problems can arise when results obtained upon different experimental conditions are correlated. In this way, Kapusta and Hackerman [6,12] relate that the composition and thickness of the film formed onto tin strongly depend on experimental conditions.

In the potentiodynamic profile recorded for a scan rate of $v = 0.2\ \mathrm{V\,s^{-1}}$, between the lower and upper scan limits $E_{\lambda c} = -1.8$ V and $E_{\lambda a} = 1.0$ V the well-defined potential regions depicted are signed as I, II, III, IV and V in Fig. 1.

Region I comprises potential values lower than those involved in the main oxidation processes and they have not deserved special discussion in literature. However, it is a region highly dependent on the pre-treatment imposed to the electrode.

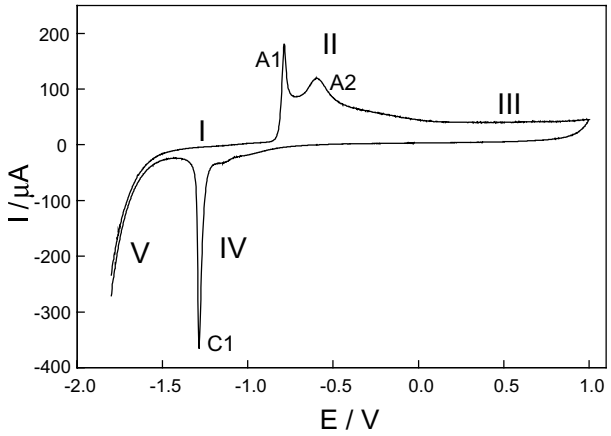

Fig. 1. Typical voltammogram of tin electrode in bicarbonate medium, 0.5 moll^{-1}, recorded at $v = 0.2$ Vs^{-1} between the limits $E_{\lambda c} = -1.8$ V and $E_{\lambda a} = 1.0$ V. Electrode A.

Region II evidenced two anodic peaks, namely A1 and A2. The presence of two peaks indicates that film formation occurs at least in two steps. The peaks correspond to the overall oxidation process $Sn \rightarrow Sn(II) \rightarrow Sn(IV)$. The formation of mixed oxides and hydroxides is possible due to the proximity of the standard equilibrium potential values for Sn/SnO and Sn/SnO_2, and for Sn/SnO and $Sn/Sn(OH)_2$.

Towards more positive potentials, in Region III, a constant current value is observed, corresponding to a passive state.

In Region IV the presence of two cathodic peaks suggests the reduction of Sn(IV) species with different electrochemical stability. A significant low cathodic charge/anodic charge relation is observed.

The presence of a current peak in Region V depends on the extent of the positive scan. In this way, a hump superimposed to hydrogen evolution current appears for a determined interval of $E_{\lambda a}$ values.

In this paper attention is focused on the Regions II and IV.

3.2. Potential domain in the proximity of peak A1

In the voltammetric curve of Fig. 2, a well-defined anodic peak at around −0.85 V, peak A1, and its cathodic counterpart peak C1, are depicted. This anodic peak was characterised by the Müller–Calandra model (also known as the layer-pore resistance model) [1] as a film growth process. Even so, a hydrodynamic contribution was manifested under rotating conditions, but it was concluded that without rotation, current at peak A1 corresponds mainly to film formation [1]. The negative going sweep resulted in the cathodic peak C1, whose maximum potential shifts towards the negative direction when $E_{\lambda a}$ increases. However, the first region of the peak profile coincides for all the voltammograms in the considered potential domain.

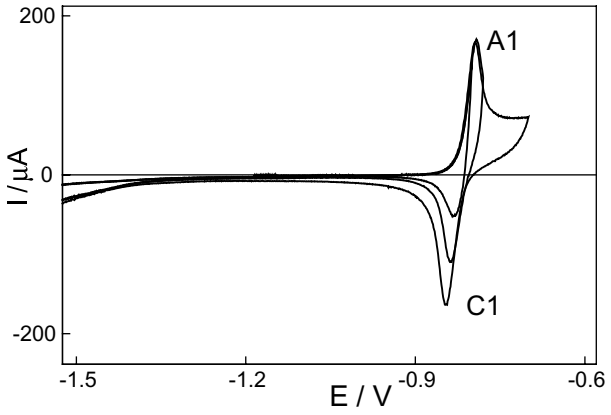

Fig. 2. Voltammograms of tin electrode, $v = 0.2\ \mathrm{V s^{-1}}$, $E_{\lambda c} = -1.8$ V, recorded for increasing $E_{\lambda a}$ values within the $-0.8/-0.7$ V interval. Electrode A.

The Nyquist plot performed at the maximum of peak A1 (Fig. 3) presents at lower frequencies an almost straight line with a $\pi/8$ slope. This behaviour can account for a heterogeneous processes diffusion limited in the pore, as it is cited in [13].

The proposed equivalent circuit is represented according the adopted nomenclature (elements that are placed in series were noted within [] and parallel elements were noted between ()). Thus, the $R(RCQ)W$ circuit is composed by a resistance-infinite length Warburg (noted as W) series combination, placed in series with three parallel branches: one corresponding to a capacitor element (noted as C), the other

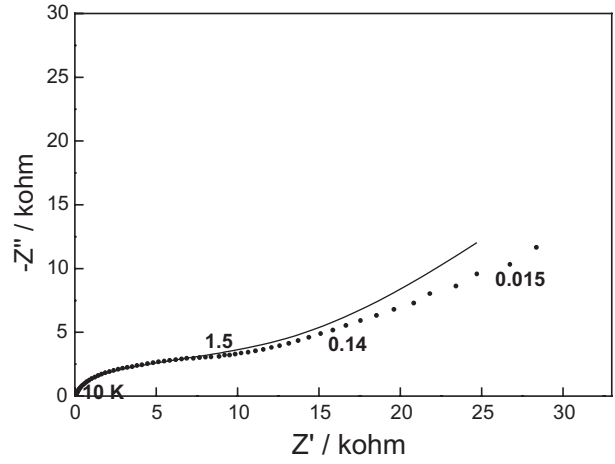

Fig. 3. Nyquist plot of the obtained data (●) for a d.c. applied potential of -0.76 V (corresponding to the maximum of peak A1). Continuous curve represents fitted results. Electrode B.

containing a resistance (noted as R), and the last with a constant phase element CPE (noted as Q according to the adopted nomenclature).

The impedance of the constant phase element Z_{CPE}, is described by the expression:

$$Z_{CPE} = [Q(j\omega)^n]^{-1}$$

where Q is a constant, combination of properties related to both the surface and the electroactive species. The parameter n is also a constant that can assume different values in the range from −1 to 1. The CPE arises from the presence of heterogeneities at the electrode–electrolyte interface, from the effect of the surface coverage on the electrode capacity or from no uniform diffusion. When $n = 0.5$, it describes an infinite length Warburg component.

Two situations were selected to be compared: the peak maximum (at −0.77 V) and a value in the descendent side of the voltammetric peak (at −0.75 V). The comparison was considered useful in order to obtain information about the nature of the anodic dynamic process and the progress of film formation. The parameters values, evaluated from the fitting procedure, are listed in Table 1.

The values of C, determined from the best fitting routine and listed in Table 1, account for metal/film/electrolyte system, giving a value of the order of 30 $\mu F\,cm^{-2}$.

The Warburg impedance accounts for the semi-infinite diffusion of the charging species. Thus, considering OH^- as the exclusive electroactive species, and the value of W from Table 1, the diffusion coefficient is extracted from the following expression [14]:

$$[W\sqrt{2}]^{-1} = \frac{RT}{n^2F^2c\sqrt{2D}}$$

The D value of the order of 10^{-5} cm^2s^{-1} obtained clearly indicates that this branch of the circuit corresponds to a diffusion process in the liquid phase.

This observation is in agreement with measurements carried out with rotating disk electrodes in the same electrochemical system [1]. In that work, it was observed a Levich's dependence between A1 current and the rotation rate, ω. Even so, the positive value of peak current at $\omega = 0$ was attributed to the contribution of current only related to the porous film formation (and modelled according to Müller–Calandra model [15,16]), leading to a control that could not be considered as only diffusional.

Table 1
Results of the impedance spectra of tin obtained from fitting as a function of the applied potential (peak A1 potential window), electrode B

E (V)	EC*	R_Ω (Ω)	$C \times 10^9$ (F)	$Q \times 10^{12}$ ($\Omega^{-1}s^n$)	n	R (kΩ)	$W \times 10^4$ ($\Omega^{-1}s^{0.5}$)
−0.77 (A1)	$R_\Omega(CQR)W$	127	243	0.09	0.35	16.3	2.37
−0.75 (A1)	$R_\Omega(CQR)W$	163	266	0.40	0.41	15.9	1.27
−0.79 (C1)	$R_\Omega(CQR)W$	187	482	131.5	0.47	73.2	0.63

* Corresponds to equivalent circuit.

For impedance measurements, the presence of various parallel branches in the equivalent circuit and the lack of a clear predominance of one of them at the intermediate frequencies domain resembles the same mixed controlled situation found at voltammetric conditions.

It is important to note that both techniques are carried out under different conditions. Thus, whereas the impedance is a potentiostatic technique, voltammetry is a potentiodynamic one. Even so, some conclusions can be scaled from the careful comparison between the results.

The resistance presented at one of the parallel branches of the equivalent circuit was considered as the charge transfer resistance. Practically the same R value observed for the two presented situations, enabling to conclude that the kinetic step is not the limiting step rate in the process.

The constant phase element presents low n values, fact that provides resistive or dissipative characteristics to the element. Values of n around 0.3 were cited in the literature in the case of porous electrodes [17]. The CPE was attributed to a distributed diffusion element, related to the energy dissipation among the porous of various sizes [17].

The increase of R_Ω value for the impedance spectrum carried out at -0.75 V can account for inclusion of the contribution of the electronic resistance of the film and/or the resistance of electrolyte in the pores of the film.

Thus, important information about the characteristics of the formed film and about the complex processes occurring were concluded. The resistive characteristic of the film was emphasised as well as the inhomogeneity, probably due to pores presence. Impedance results indicate that two main diffusion processes can be combined to account for the A1 process: ionic diffusion in liquid phase and diffusion inside the porous film.

The study of the reduction profile not only enables the characterisation of the cathodic processes but also complements the information about the anodic behaviour since everything that occurs in the positive profile is reflected in the negative scan.

The Nyquist plot obtained from impedance results at peak C1 maximum and the fitted results according to the use of the equivalent circuit: $R(CQR)W$ are shown in Fig. 4.

The best data fitting results from the equivalent circuit are listed in Table 1. Also three branches are presented. C is attributed to the metal/film/electrolyte capacitance. The lower C value compared to anodic process accounts for the thickness of the not completely reduced, remanent film. R, corresponding to transfer charge resistance shows a value almost six times higher than that for the corresponding anodic process. The existence of the remanent oxide film can also contribute to the increase of R, when compared again with the fitted parameters for the anodic process.

Two diffusion contributions are involved in the cathodic processes. At the lower frequency domain, the $\pi/4$ slope is associated to a Warburg impedance. The value of W is indicative of a diffusion process occurring in liquid phase. On the other side, the exponent of the CPE component indicates another diffusion contribution, but more pronounced at intermediate frequencies and occurring in or on solid phase. The

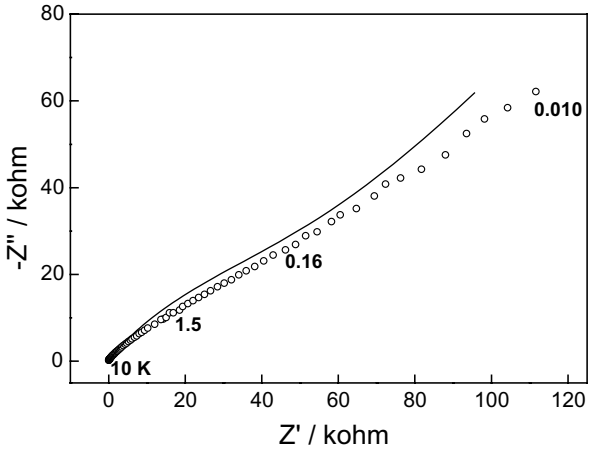

Fig. 4. Nyquist plot of the obtained data (○) for a d.c. applied potential of −0.79 V (corresponding to the maximum of peak C1). Continuous curve represents fitted results. Electrode B.

latter can be related to diffusion process along the surface producing bulk metal from the nuclei. These results sustained by those obtained from voltammetric measurements drive the interpretation towards the following conclusion: film reduction occurs through electronic transport from the underlying metal to the film/solution interface [18]. The influence of the variation of the lower scan potential limit on the subsequent anodic current profile is shown in Fig. 5. The cathodic sweep was reversed at various degrees of the oxide reduction; the current that flow upon reoxidation of the partially reduced film depends on the area of the removed film (Fig. 5).

3.3. Potential domain in the proximity of peak A2

In the voltammetric curve of Fig. 6 the anodic peak A2 and its counterpart, the cathodic peak C1 are observed. At this peak the growing of the film, was interpreted [1] according to the model proposed by Müller–Calandra. It was evidenced the same mathematical relationship of A1 peak as a consequent of rotation. Probably the same species exert the diffusional control of both the processes, A1 and A2 [1]. The negative going sweep resulted in one cathodic peak accounting for the reduction of A1 and A2, which shifts towards negative direction when $E_{\lambda a}$ increases.

The impedance spectrum, determined at the maximum of peak A2, is quite complex (Fig. 7), suggesting that multiple parallel reactions occur on the electrode. A higher frequency loop is followed by a linear portion, which passes into a negative resistance region. The most common source of negative resistance results from an interplay between adsorption and electrodissolution, giving rise to a current that decreases with increasing voltage for frequencies $\rightarrow 0$.

The presence of dissolution processes was evidenced in voltammetric measurements involving peak A2 region [19]. At low scan rates, the negative sweep showed

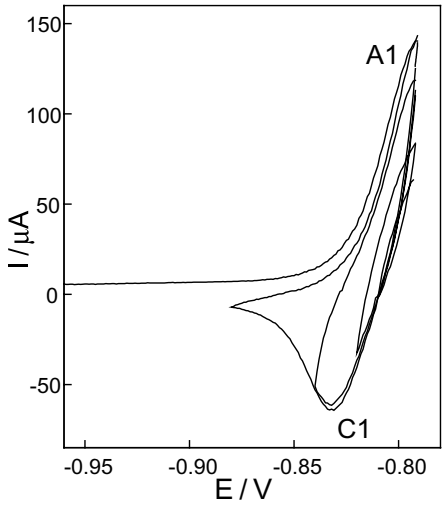

Fig. 5. Voltammetric profiles in the potential window of A1 and C1, $E_{\lambda a} = -0.79$ V and with decreasing values of $E_{\lambda c}$ between -0.88 and -0.82 V, $v = 0.2\ \mathrm{V\,s^{-1}}$. Electrode A.

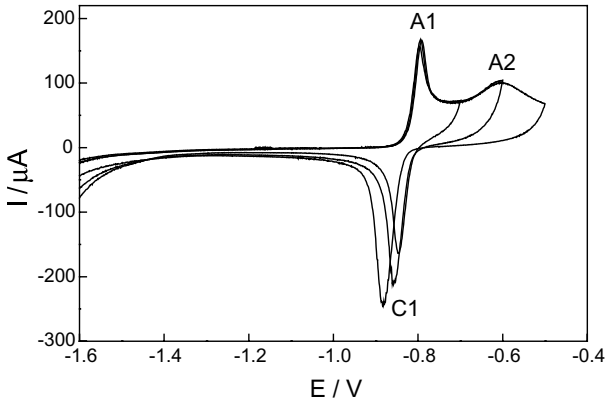

Fig. 6. Voltammograms for tin electrode, $v = 0.2\ \mathrm{V\,s^{-1}}$, $E_{\lambda c} = -1.8$ V, recorded for increasing $E_{\lambda a}$ values within the $-0.7/-0.5$ V interval. Electrode A.

an unexpected profile of positive currents, that was interpreted as a re-activation process.

The equivalent circuit has the form: $R(CR)(QR)$ and the fitted curve is shown in Fig. 7. Table 2 presents the values of the elements considered in the equivalent circuit. C was assigned to metal/film/electrolyte capacitance and R_1 accounts for the charge transfer resistance. The value of n so far from 1 can be interpreted as the presence of an irregular surface.

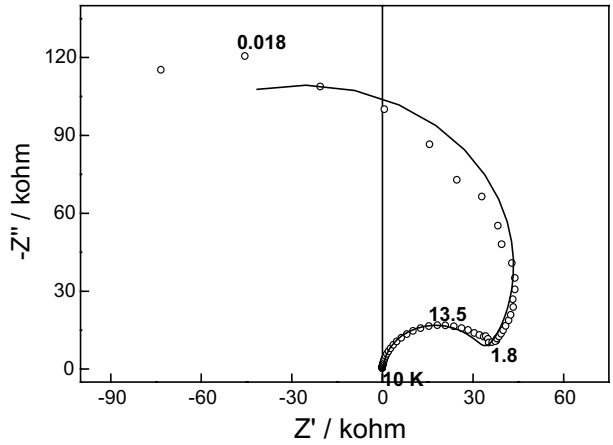

Fig. 7. Nyquist plot of the obtained data (○) for a d.c. applied potential of −0.6 V (corresponding to the maximum of peak A2). Continuous curve represents fitted results. Electrode B.

Table 2
Results of the impedance spectra of tin obtained from fitting as a function of the applied potential (peak A2 potential window), electrode B

E (V)	EC*	R_Ω (Ω)	$C \times 10^9$ (F)	R_1 (kΩ)	$Q_1 \times 10^7$ ($\Omega^{-1} s^n$)	n_1	R_2 (kΩ)	$Q_2 \times 10^7$ ($\Omega^{-1} s^n$)	n_2
−0.60 (A2)	$R_\Omega(CR_1)(QR_2)$	171	296	30.9	0.53	0.62	−114.8		
−0.817 ($C1_a$)	$R_\Omega(CQ_1R_1)Q_2$	176	933	206	296.9	0.48		0.798	0.59

* Corresponds to equivalent circuit.

The cathodic peak C1, showed an atypical impedance spectrum. The Bode plot in the form $\log(Z)$ vs. $\log(f)$ evidenced three frequency domains, separated by drastic jumps resulted from discontinuity. The presence of the intermediate portion with higher impedance values may suggest the occurrence of a drastic change in the electrical nature of the film. In this case, the total impedance increase accounts for decrease in conductivity. The good reproducibility of the results show that this breaking point can be ascribed to a change in the nature of the charge transfer conductivity of the tin film.

Sometimes, the incipient formation of a new phase in the oxide matrix can introduce an increase in resistance due to a less efficient intergrain conduction. However, it is important to notice that peak C1 is formed by the combination of two current contributions (which depend on time variable) rather than the result of a single process, as it will be presented later. In this way, a simple impedance response is not expected to occur in potential regions which presents such process complexity.

It has been observed that when the electrode was subjected to a potentiostatic ageing procedure in the region of peak A2, its counterpart, peak C1, split into two current contributions which were evidenced as two shoulders (Fig. 8). The current

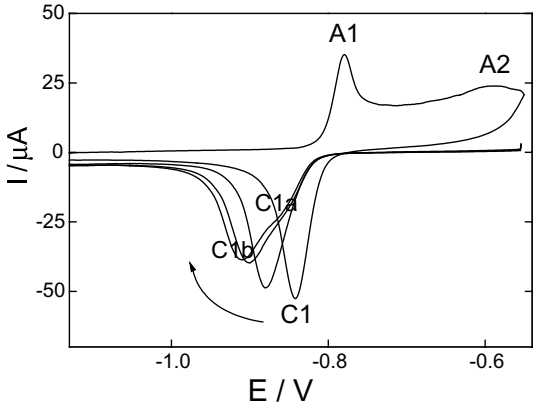

Fig. 8. Voltammograms recorded at $v = 0.2\ V\,s^{-1}$ between the limits $E_{\lambda c} = -1.8$ V and $E_{\lambda a} = -0.55$ V. The typical cathodic profile is compared with profiles recorded after a potentiostatic ageing procedure at −0.55 V for increasing times τ: 30 s, 1, 3 and 5 min. Electrode B.

contributions can be completely separated into two well-defined peaks for ageing times longer than 5 min. The potentiostatically aged film presents at least two states with different stabilities, being the most stable one reduced at more negative values.

In order to organise data presentation, the two current contributions will be named as $C1_a$(the less negative peak) and $C1_b$ (the more negative peak). The separation between $C1_a$ and $C1_b$ increases with τ, whereas $C1_b$ charge slightly increases in detriment of $C1_a$ charge [19].

Impedance measurements performed at $C1_a$ immediately after the potentiostatic ageing procedure with τ values of 15 and 30 min presents the Nyquist plots of Fig. 9. On the other side, the diagrams obtained after $\tau = 5$ min shows discontinuities that resembles the spectra recorded for the cathodic peak C1 without the application of the ageing procedure. Since the two current contributions were not completely isolated at $\tau = 5$ min, it seems logic that results exhibit characteristics comparable to those of the peak C1.

The Nyquist diagrams corresponding to surfaces subjected to ageing procedures of 15 and 30 min are practically identical. Parameters evaluation from the EC fitting are listed in Table 2. Q_2 can be practically assigned to a semi-infinite Warburg element. Q_1 presents also strong characteristics of a Warburg element. Q_1 and Q_2 account for diffusion in solid phase, indicating the occurrence of a solid phase process. The principal effect resulted from the ageing procedure was the increase of C value. This can account for the presence of a remanent oxide film, not completely reduced at the electrode surface. It is important to remember that the most stable portion of the aged film is only reduced at more negative potentials.

Impedance measurements performed at the maximum of $C1_b$ showed a Bode plot $\log(Z)$ vs. $\log(f)$ which evidenced three frequency domains as it was shown in the C1 Bode spectrum. It seems clear that the responsible for the ''atypical'' profile in the C1 spectra is the $C1_b$ contribution.

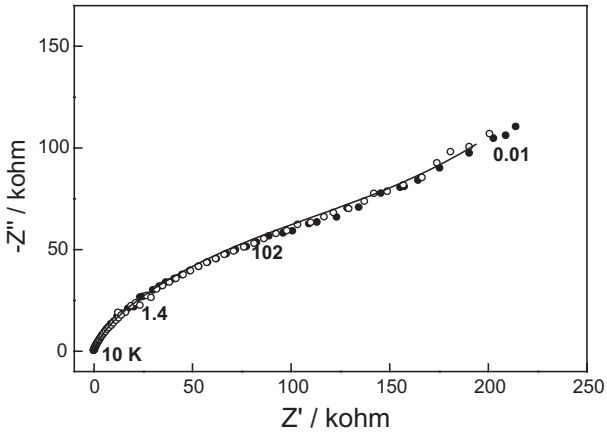

Fig. 9. Nyquist plot of the obtained data for a d.c. applied potential of: −0.817 V (open circle, corresponding to the maximum of peak $C1_a$ after an ageing procedure of 15 min) and −0.813 V (solid circle, corresponding to the maximum of peak $C1_a$ after an ageing procedure of 30 min). Continuous curve represents fitted results according to the use of the equivalent circuit. Electrode B.

The log(f) vs. log(Z) plot measured for the aged surfaces displays discontinuities. In Fig. 10, the plot for $\tau = 15$ min is shown. The shape of the spectrum of Fig. 10 resembles the simulated ones corresponding to potential values sufficiently close to transition potentials, when the frequency sweep direction is from high to low values [20]. There is cited [20] that the Faradaic impedance magnitude varies in a discontinuous way for the transition potential and that it is theoretically possible to measure an impedance diagram for a potential as close as that required for the bifurcation, by

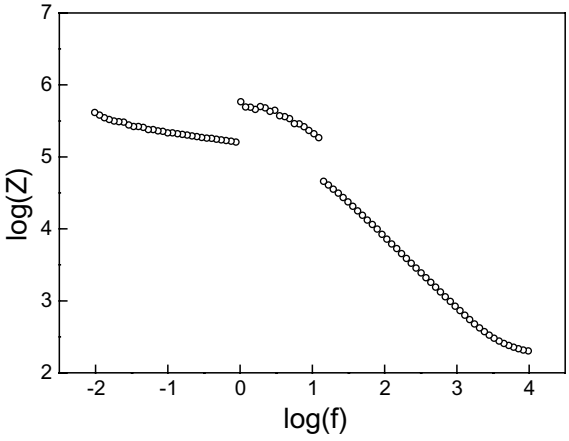

Fig. 10. Bode plot of the obtained data for the d.c. applied potential of −0.906 V (corresponding to the maximum of peak $C1_b$). Electrode B.

choosing a sufficiently small sinusoidal signal amplitude. Therefore, by assuming that the potentials selected to carry out the impedance measurements (maximum of peak $C1_b$) were close enough to a static bifurcation point, it is likely at least at a theoretical point of view to obtain a diagram with the characteristics of that of Fig. 10.

The presence of a discontinuous transition point is possible in the present system. But to sustain this hypothesis a brief review about the system response against ageing procedure application should be offered. Although only some results from application of potentiostatic ageing procedure are discussed here, results from potentiodynamic ageing procedures are necessary to sustain the interpretation [19]. Even so, as their discussion is beyond the scope of the paper (more related studies are now in progress) only the useful and strictly pertinent conclusions are drawn out. In this way, the solely imposition of an ageing time τ, *per se*, does not entirely control the extent of the ageing process or namely, the average energetic configuration of the surface species. There is another controlling component concerning time-evolution of the more stable reduced species (those reduced at $C1_b$) and the interconversion between the aged species ($C1_a$ and $C1_b$), which depends on perturbation characteristics (amplitude and frequency), as results of potentiodynamic ageing procedures showed [19]. Thus, potentiostatic time τ acts imposing the ageing extent of the formed film, and thus, establishing the reduction potential of the two different stability species (and consequently imposing the potential of $C1_a$ and $C1_b$). But, the interconversion between $C1_a$ and $C1_b$ species and the simultaneous time-evolution extent of species in $C1_b$, depend on the nature of applied perturbation. It is possible to correlate the presence of multi-states and the different extent of time-evolution of the $C1_b$ species. So, the discontinuous transition point is related to the passage of the stable steady-state (initial state) to differently aged reduced species. Obviously, this dynamical behaviour was only evidenced due to the positive correlation of experimental parameter values (sweep frequency direction, modulation amplitude, selected potential) [21] and intrinsic parameters of the system (interconversion and time-evolution rate constants).

As this is a complex topic and deserves more discussion, related studies are now in progress.

4. Conclusions

The electrochemical behaviour of potentiodynamically formed anodic tin films in sodium bicarbonate solutions were studied by cyclic voltammetry and electrochemical impedance spectroscopy. Different equivalent circuits corresponding to various potential regions were employed to account for the electrochemical processes taking place under each condition.

Two main factors are determining the extent of the ageing process. One of them arises from the imposition of a potentiostatic ageing time. The other factor is related to the time-evolution of the more stable reduced species, which depends on both time and perturbation characteristics. The relation between the different species and the

subsequent evolution extent, depend on time and nature of applied perturbation. The correlation of each degree of this species evolution can be assigned to multi states. Therefore, the observed discontinuous transition is related to the passage of the stable initial state to different degree aged reduced species.

Acknowledgements

J.R. wishes to thank CSIC (UDELAR, Universidad de la República, Uruguay) for the fellowship granted. FAPESP (Fundação de Amparo à Pesquisa do Estado de São Paulo, Brasil) 93333-2 is gratefully acknowledged.

References

[1] S.H. Bonilla, B.F. Giannetti, Z. Phys. Chem. 218 (2004) 837.
[2] C.M.V.B. Almeida, B.F. Giannetti, T. Rabockai, J. Electroanal. Chem. 422 (1997) 185.
[3] State of California Department of Health Services, Determination of perchlorate by ion chromatography, Rev. No. 0, 7th May 1997.
[4] A.J. Arvía, Israel J. Chem. 18 (1979) 89.
[5] B.A. Boukamp, EQUIVCRT TM Software, University of Twente, Department of Chemical Technology, P.O. Box 217, 7500 AE Enschede, The Netherlands.
[6] S.D. Kapusta, N. Hackerman, Electrochim. Acta 25 (1980) 1625.
[7] A. Vértes, H. Leidheiser, M.L. Varsányi, G.W. Simmons, L. Kiss, J. Electrochem. Soc. 125 (1978) 1946.
[8] M.L Varsányi, J. Jaén, A. Vértes, L. Kiss, Electrochim. Acta 30 (1985) 529.
[9] M. Metikoš-Huković, M. Šeruga, S. Ferina, Ber. Bunsenges. Phys. Chem. 96 (1992) 799.
[10] M. Drogowska, L. Brossard, H. Menard, J. Electrochem. Soc. 138 (1991) 1243.
[11] C.A. Gervasi, F.E. Varela, J.R. Vilche, P.E. Alvarez, Electrochim. Acta 42 (1997) 537.
[12] S. Kapusta, N. Hackerman, Electrochim. Acta 25 (1980) 1001.
[13] C. Gabrielli, Identification of electrochemical processes by frequency response analysis, Technical report number 004/83, Solartron Instruments, 1980.
[14] R. Greef, R. Peat, L.M. Peter, D. Pletcher, J. Robinson, Instrumental Methods in Electrochemistry, Ellis Horwood Limited, Chichester, 1985 (Chapter 8).
[15] W.J. Mueller, Trans. Faraday Soc. 27 (1931) 737.
[16] A.J. Calandra, N.R. Tacconi, R. Pereiro, A.J. Arvía, Electrochim. Acta 19 (1974) 901.
[17] Deyang Qu, Electrochim. Acta 48 (2003) 1675.
[18] D. Williams, Electrochim. Acta 21 (1976) 1097.
[19] S.H. Bonilla, Doctoral thesis, University of São Paulo, São Paulo, Brazil, 2001.
[20] F. Berthier, J.-P. Diard, C. Montella, J. Electroanal. Chem. 410 (1996) 247.
[21] F. Berthier, J.-P. Diard, C. Montella, 10ème Forum sur les Impédances Electrochimiques, Paris, 1995, p. 235.